*CHINA PARTICUOLOGY Vol. 1, No. 5, 219–222, 2003*

● ***Instrument***

# PROTEIN CHARACTERIZATION USING DYNAMIC AND STATIC LIGHT SCATTERING

Jeffrey Yang[1,*] and Kevin Mattison[2]

[1]*SiberHegner China Ltd., 26/F West Tower, Hanwei Plaza, No.7 Guanghua Road, Beijing 100004, P. R. China*
[2]*Malvern Instruments Inc., 10 Southville Road, Southborough, MA01772, USA*
**Author to whom correspondence should be addressed. E-mail: jeffrey.yang@siberhegnerchina.com*

## Introduction

The stability of a protein formulation to a variety of solution perturbations is critical to its success as a pharmaceutical product. Because of the sensitivity of the protein to solution changes, invasive characterization techniques can be problematic. Light scattering is a non-invasive technique that has received wide acceptance in the area of protein formulation and characterization.

The scattering intensity of a small molecule is proportional to the square of the molecular weight. As such, dynamic and static light scattering techniques are very sensitive to the onset of protein aggregation arising from subtle changes in the solution conditions. Today's generation of light scattering instrumentation includes high powered power lasers, fiber optics, high speed correlators, and single photon counting detectors that facilitate the measurement of protein samples across a range of size and concentration that has never before been achievable.

## Light Scattering Measurements (SLS and DLS)

The dynamic light scattering (DLS) technique was used to determine the hydrodynamic size of a single molecule and the aggregates of protein in solution (Chu, 1991; Berne & Pecora, 1976). Standard analysis methods such as the double-exponential sampling method, exponential sampling method, second-order cumulant method, and CONTIN were used to determine the particle radius (Chu, 1991; Berne & Pecora, 1976). The DLS data were collected at a fixed scattering angle.

The static light scattering (SLS) technique was used to determine the molecular weights and radii of gyration of the single molecule and the aggregates of protein. The data analysis of SLS was done by using the Zimm equation (Zimm,1948a; Zimm, 1948b):

$$\frac{KC}{\Delta I(\theta)} = \left(\frac{1}{M_w} + 2A_2C\right)\left(1 + \frac{16\pi^2 n_0^2}{3\lambda_0^2}\overline{\langle R_g^2\rangle_z}\sin^2\left(\frac{\theta}{2}\right)\right), \quad (1)$$

which relates excess scattering from the polymer solution $\Delta I(\theta)$ to the polymer concentration $C$ and the scattering angle $\theta$ to determine $M_w$, $R_g$, and the modified second virial coefficient $A_2$. The constant $K$ accounts for the experimental parameters such as the scattering volume, $V$, the distance from the scattering center to the detector, $r$, and the increment in refractive index with concentration d$n$/d$C$:

$$K = \frac{4\pi^2 n_0^2}{\lambda_0^4 N_A}\left(\frac{dn}{dC}\right)^2 \frac{I_0 V}{r^2}, \quad (2)$$

where $n_0$ is the solvent refractive index, $\lambda_0$ is the wavelength of the incident light, $N_A$ is the Avogadro number, and $I_0$ is the incident laser intensity. Calibration using toluene, for which the reported Raleigh ratio is $r^2 I(90°)/VI_0 = 4.0\times10^{-5}\text{cm}^{-1}$, $V/r^2$ is determined. To analyze SLS data, $\Delta I(\theta)$ was measured at several concentrations and angles. The usual Zimm plot was then constructed by plotting $KC/\Delta I(\theta)$ as a function of $\sin^2(\theta/2)+k'C$, as shown in Fig. 1, where $k'$ is an arbitration constant. Extrapolating $KC/\Delta I(\theta)$ to zero angle or zero concentration determined $M_w$, $R_g$, and $A_2$. Both $R_g$ and the molecular weight of protein or polymers were determined by DLS and SLS. In applying the standard Zimm plot, one usually assumes that polymer molecules do not aggregate with increasing concentration (Stacy, 1956; Lang & Burchard, 1993; Schmitz, 1990).

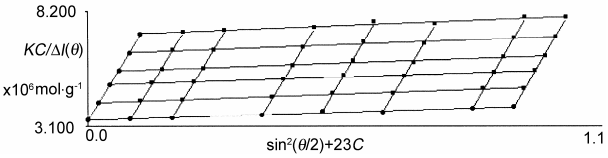


Fig. 1 Zimm plot.

## Thermal Denaturation

The structure of a protein is stabilized by a large number of hydrogen bonds, hydrophobic interactions, and van der Waal forces, each of which contributes a small degree of stability to the overall structure. As energy is added to the system via an increase in temperature, the stabilizing forces can be disrupted, allowing the protein to unfold or denature. The temperature at which this denaturation occurs is defined as the protein melting point.

When a protein denatures, the hydrophobic residues buried within the interior of the folded structure are exposed to the solvent. This entropically unfavorable state is soon replaced, however, with one wherein the hydropho-

bic residues on one protein chain associate with those on another protein chain. Because of the molecular weight dependence of the scattering intensity, this non-specific aggregation of denatured proteins is easily monitored with light scattering instrumentation. Fig. 2 shows a temperature scan for bovine hemoglobin, and clearly indicates a sharp increase in both the size and scattering intensity at the melting point of 45.5℃.

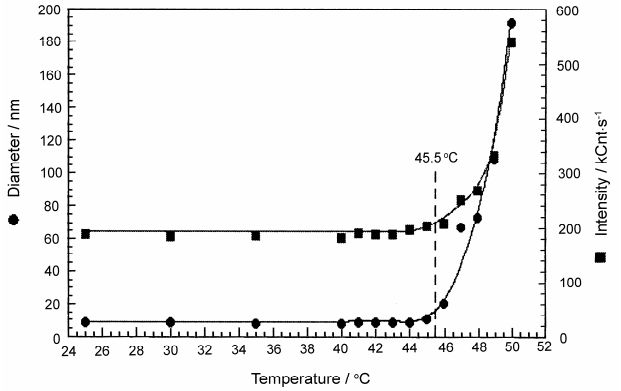


Fig. 2 Thermal scan for bovine hemoglobin in 0.13 M phosphate buffered saline, indicating a melting point of 45.5℃.

## Quaternary Structure

The quaternary structure or ordered self-association state of a protein can be influenced by solution properties. Precision in dynamic light scattering (DLS) measurements is sufficient to distinguish changes in protein quaternary structure. For example, Fig. 3 shows the measured size distributions for human and bovine insulin at pH 2 and pH 7. At pH 2, the measured diameters for both proteins (see Table 1) are consistent with dimeric quaternary structures, where the molecular weight is estimated from empirically determined size vs. mass relationships. At pH 7, the measured diameters are consistent with the known hexameric forms of the proteins at physiological pH.

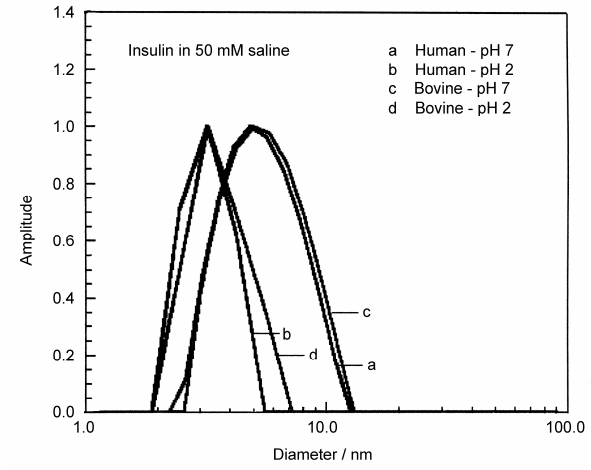


Fig. 3 Size distributions for human and bovine insulin at pH 7 and pH 2, indicating a pH dependent change in quaternary structure.

Table 1 Comparison of the pH dependent calculated and known molecular weight values for human and bovine insulin

| | pH | Diam / nm | $M_{Et}$ / kDa | $M_{Known}$ / kDa | Form |
|---|---|---|---|---|---|
| Human | 2 | 3.30 | 10.9 | 11.4 | Dimer |
| | 7 | 5.37 | 33.9 | 34.2 | Hexamer |
| Bovine | 2 | 3.47 | 12.2 | – | Dimer |
| | 7 | 5.33 | 33.4 | – | Hexamer |

## Non-specific Aggregation

Formulation additives can have a pronounced influence on the surface charge density of the protein and the solution ionic strength. Subtle variations in either of these parameters can mean the difference between a stable formulation and sample aggregation. Because of its sensitivity to high molecular weight particles, DLS is a useful tool for monitoring the effects of formulation additives on protein aggregation.

Fig. 4 shows an overlay of the size distribution for bovine serum albumin as a function of ionic strength at the isoionic point of pH 4.8. For NaCl concentrations $< 0.5$ M, the size distribution in monomodal, with a hydrodynamic diameter of circa 8.5 nm. For NaCl concentrations $\geq 0.5$ M, the size distribution is multi-modal, indicating the presence of protein aggregation.

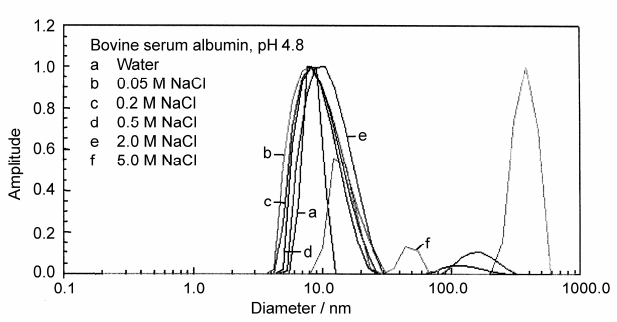


Fig. 4 Size distribution results for bovine serum albumin at pH 4.8 as a function of NaCl concentration. Aggregation is indicated at NaCl concentration $\geq 0.5$ M.

## Molecular Weight and Virial Coefficient

For small molecules such as proteins, the sample scattering intensity can be described using the Rayleigh expression shown in Eq. (3) (Debye, 1947):

$$\frac{KC}{R_\theta} = \frac{1}{M} + 2A_2C\,, \qquad (3)$$

where $K$ is an optical constant, $C$ is the protein concentration, $R_\theta$ is the Rayleigh ratio of the analyte intensity to the incident intensity, $M$ is the molecular weight of analyte in weight average, and $A_2$ is the 2nd virial coefficient.

As suggested in Eq. (3), a plot of $KC/R_\theta$ vs. $C$ should be linear, with an intercept equivalent to $1/M$ and a slope that is proportional to the 2nd virial coefficient. This type of single angle molecular weight analysis is known as a Debye plot (Debye, 1947), as shown in Fig. 5 for lysozyme

in 0.1 M acetic acid buffer and 0.13 M phosphate buffered saline. The intercepts in both plots are consistent with the known molecular weight of 14.7 kDa. As seen in Fig. 5, however, the 2nd virial coefficients are strongly dependent upon the type of buffer used.

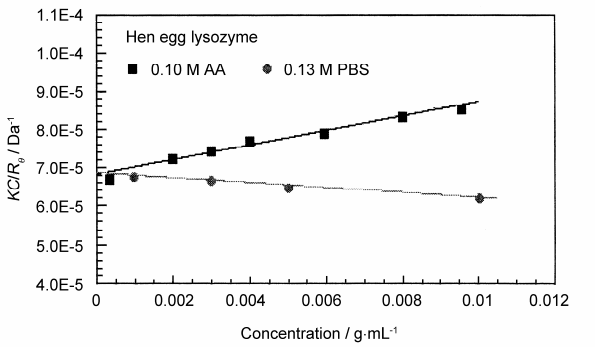


Fig. 5 Debye plots for lysozyme in 0.10 M acetic acid buffer and 0.13 M phosphate buffered saline.

## Shape Estimates

In dynamic light scattering measurements, the hydrodynamic size is calculated from the measured diffusion coefficient via the Stokes-Einstein equation (Chu, 1991; Berne & Pecora, 1976), where a hard sphere model is assumed. Deviations in sphericity are reflected in an increase in the hydrodynamic size compared to the size calculated for a hard sphere of known molecular weight. From Perrin theory (Schumacher, 1986), the difference between these two values, i.e. hydrodynamic size and the hard sphere size, can be used to estimate the axial ratio for an ellipsoid with the same diffusional properties. Fig. 6

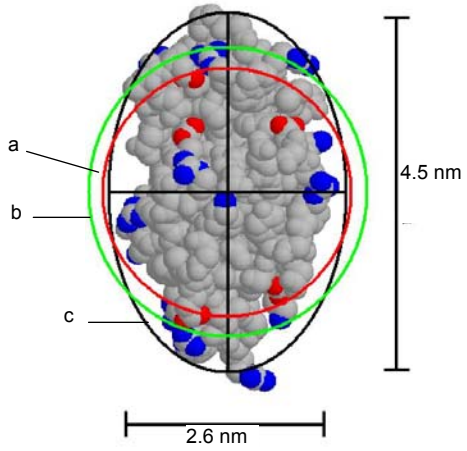


Fig. 6 Representation of lysozyme, showing the geometric axial dimensions, the hard sphere diameter (a), hydrodynamic diameter (b), and an ellipsoid with the same diffusional properties as the protein (c).

shows a representation of the crystal structure for lysozyme, and includes the geometric axial dimensions. The circle a is representative of the size of a hypothetical hard sphere for the 14.7 kDa protein (specific volume=0.73 $mL \cdot g^{-1}$). The circle b is representative of the hydrodynamic size, calculated from the measured diffusion coefficient. The difference between the measured and theoretical values is consistent with an ellipsoid particle shape with an axial ratio of 1.73, identical to the axial ratio determined geometrically.

## Zetasizer Nano ZS

Launched in May this year, the Zetasizer Nano ZS, as shown in Fig. 7, measures particle size, zeta potential and molecular weight all within one fully automated and highly versatile unit. This article characterization system has won Instrument Business Outlook's (IBO) 2003 Gold Award for excellence in industrial design of analytical and life science instruments. Table 2 lists its specificastions.

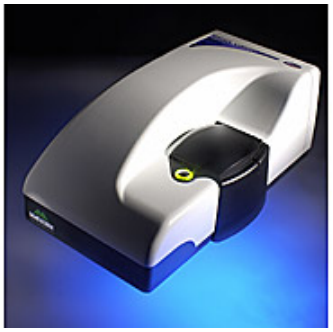

Fig. 7 Zetasizer Nano ZS, Malvern Instruments Ltd.

Table 2 Specifications of Zetasizer Nano ZS, Malvern Instruments Ltd.

| | |
|---|---|
| Size, zeta potential and molecular weight, measurement of particles, emulsions and molecules | |
| **Size measurement** | |
| Size range | 0.6 nm~6 microns* |
| Minimum sample volume | 12 microlitres |
| Concentration range | 0.1 $mg \cdot mL^{-1}$ lysozyme to 40% W/V* |
| **Zeta potential measurement** | |
| Minimum sample volume | 0.75 mL |
| Maximum sample conductivity | 200 mS |
| **$M_w$ measurement** | |
| Molecular weight range | $1\times10^3$ to $2\times10^7$ Da* |
| Minimum sample volume | 20 microlitres |
| Minimum sample volume for automated measurement using MPT-2 autotitrator | 3 mL |
| **Automated trend measurement** | |
| Standard software | Time and temperature |
| Using optional MPT-2 autotitrator | pH, conductivity or additive |
| **General specifications** | |
| Temperature control | 2℃ to 90℃ |
| Condensation control | Purge facility using dry air/nitrogen |
| Laser | 4 mW He–Ne, 633 nm |
| Product laser class | Class 1 compliant, EN 60825-1:2001 and CDRH |
| Size | 320 mm, 600 mm, 260 mm (W,D,H) |
| Weight | 18 kg |

* Sample depended.

Based on the HPPS using the NIBS principle (Non-invasive Back-Scattering) (Yang, 2003), Zetasizer Nano ZS from Malvern Instruments was specifically designed to meet the low concentration requirements typically associated with protein applications, along with the high concentration requirements for other colloidal applications. Satisfying this unique mix of requirements was accomplished via the integration of a backscatter optical design, and as a consequence of this design, the specifications far exceed those for any other dynamic light scattering instrument. The hardware is self-optimizing, and the software includes a unique "one click" measure, analyze, and report feature designed to minimize the learning curve (Malvern Instruments Ltd., 2003).

## Acknowledgement

The authors thank Malvern Instruments Ltd. for instrumentation and experiment help.

## References

Berne, B. J. & Pecora, R. (1976). *Dynamic Light Scattering: with Application to Chemistry, Biology and Physics* (1st ed.). New York: Wiley.

Chu, B. (1991). *Light Scattering: Basic Principle and Practice* (2nd ed.). San Diego: Academic Press.

Debye, P. (1947). Molecular-weight determination by light scattering. *J. Phys. Colloid Chem.*, 51, 18–32.

Lang, P. & Burchard, W. (1993). Structure and aggregation behavior of tamarind seed polysaccharide in aqueous solution. *Makromol. Chem.*, 194, 3157–3166.

Malvern Instruments Ltd. (2003). Zetasizer Nano ZS brochure. http:\\www.Malvern.co.uk.

Schmitz, K. S. (1990). *An Introduction to Dynamic Light Scattering by Macromolecules* (1st ed.). Boston: Academic Press.

Schumacher, R. T. (1986). Brownian motion by light scattering revisited. *Am. J. Phys.*, 54, 137.

Stacy, K. A. (1956). *Light Scattering in Physical Chemistry* (1st ed.). Orlando: Academic Press.

Yang, J. (2003). Measurement of nanometer scale cadmium selenide nanocrystals and cluster molecules. *China Particuology*, 1(4), 181–182.

Zimm, B. H. (1948a). The scattering of light and the radial distribution function of high polymer solutions. *J. Chem. Phys.*, 16, 1093–1098.

Zimm, B. H. (1948b). Apparatus and methods for measurement and interpretation of angular variation of light scattering. *J. Chem. Phys.*, 16, 1099–1116.

*Manuscript received July 12, 2003 and accepted September 9, 2003.*